J Appl Electrochem (2011) 41:1287–1294
DOI 10.1007/s10800-011-0340-x

ORIGINAL PAPER

The effect of electrochemical lithiation on physicochemical properties of RF-sputtered Sn thin films

C. S. Nimisha · G. Venkatesh · N. Munichandraiah · G. Mohan Rao

Received: 30 May 2011 / Accepted: 15 July 2011 / Published online: 29 July 2011

Abstract Thin films of Sn were deposited on Pt/Si substrates by sputtering technique and subjected to electrochemical lithiation studies. Electrochemical lithiation of Sn resulted in the formation of Sn–Li alloys of different compositions. Charging of Sn-coated Pt/Si electrodes was terminated at different potentials and the electrodes were examined for physicochemical properties. The scanning electron microscopy and atomic force microscopy images suggested that the Sn films expanded on lithiation. Roughness of the film increased with an increase in the quantity of Li present in Sn–Li alloy. Electrochemical impedance data suggested that the kinetics of charging became sluggish with an increase in the quantity of Li in Sn–Li alloy.

Keywords Tin films · RF sputtering · Electrochemical lithiation · Surface roughness

1 Introduction

All-solid-state thin film battery (TFB) has gained attention because of the on-chip power requirement for microelectronic mechanical systems, low-power CMOS-based integrated circuits, radio frequency identification tags, etc. To realize a TFB, coatings of multilayer thin films including current collectors, cathode, electrolyte, anode and protective layers are required. TFB using metallic lithium as the anode layer has been reported because of its high theoretical specific capacity (3,860 mAh g^{-1}) [1–5]. Additionally, it has a high negative potential that leads to a high cell voltage. However, the major drawbacks of TFB employing metallic lithium as the anode are the following: (i) special evaporation chamber inside an argon-filled glove box is needed for Li coating by evaporation, (ii) moisture protection package is needed before air exposure and (iii) because of low melting point of Li, anode film cannot survive standard solder reflow process during circuit assembly. To avoid these problems, Sn layer was studied as an alternative anode [6–8]. Sn has a high mass and volume capacities of 994 mAh g^{-1} and 7,254 mAh cm^{-3}, respectively [9, 10]. Sn alloys with Li resulting in different compositions. The maximum Li uptake is 4.4 atoms for an Sn atom, reaching the composition of $Li_{4.4}Sn$. During charging and discharging of Sn, basically alloying and de-alloying reactions occur between Sn and Li. However, poor cycleability is associated with Sn anode. The high capacity expected from Sn anode accompanies considerable volume changes and unwanted structural modifications during alloying and de-alloying processes. The strain formed at the boundaries of the crystalline phases results in poor cyclic performance.

There are only a few reports concerning the effect of lithiation of Sn thin film electrodes [11, 12]. In this study, thin films of Sn are deposited on Si substrates by radio frequency (RF) sputtering technique. A highly porous film with nano features is obtained by this method that results in a high surface area. Electrochemical lithiation is carried out to different stages and the electrodes are examined by several physicochemical techniques. Physical and chemical changes occurring as a result of lithiation are analyzed in detail. The results suggest that the films become progressively

C. S. Nimisha (✉) · G. Mohan Rao
Department of Instrumentation and Applied Physics, Indian Institute of Science, Bangalore 560012, India
e-mail: nimishacs@yahoo.com

G. Venkatesh · N. Munichandraiah
Department of Inorganic and Physical Chemistry, Indian Institute of Science, Bangalore 560012, India

pulverized resulting in increased roughness with an increase in lithiation.

2 Experimental procedures

Sn thin films were prepared by RF sputtering from a Sn target (99.99% purity of 3" diameter) at 5×10^{-3} mbar pressure. The RF power used was 60 W with an Ar flow of 40 sccm and the depositions were carried out at room temperature for 10 min. The thickness of Sn films is found to be ~ 2 μm. Thickness can be increased by increasing the time of sputtering. But experiments were carried out with films deposited for 10 min in this work. Pt-coated Si strips of the required size for electrochemical studies (0.8×2.0 cm) and for other characterization (1.0×1.0 cm) were used as substrates. The crystal phases and microstructure of the thin film electrodes were characterized by X-ray diffraction (XRD) and scanning electron microscopy (SEM) using a Bruker D-8 Advance diffractometer with Cu Kα radiation and a SIRION FE-SEM microscope, respectively. The composition of the sample was analyzed by energy dispersive spectroscope (EDX) with an INCA300 EDS attached to SEM. The surface chemical composition of Sn electrode was estimated using X-ray photoelectron spectroscopy (XPS) (SPECS-Phoibos 100 MCD Energy Analyzer) using MgKα radiation (1,253.6 eV). The quantification of Sn and Li at different lithiation potential was determined by quantitative XPS analysis using CASA XPS software. The surface morphology and roughness changes during lithiation to different potentials were investigated with the help of a Nanosurf Easy Scan2 atomic force microscope (AFM) (Nanosurf AG, Switzerland) in air at room temperature by contact mode.

The electrochemical studies of Sn thin film electrodes were carried out with Sn thin film deposited Pt/Si as the working electrode and Li foil as the counter-cum reference electrode with Celgard 2300 membrane as the separator. A concentration of 1-M $LiAsF_6$ dissolved in a mixture of ethylene carbonate and dimethyl carbonate (1:1 by vol.) was used as the electrolyte. Cells were assembled in air-tight glass containers in Ar-filled MBraun glove-box model Unilab. Cells were galvanostatically charged and discharged at 10 μA cm^{-2} using a Bio-Logic SA potentiostat/galvanostat model VPM3 within the potential range of 0.2–1.2 V (vs. Li/Li^+) at ambient temperature. Cyclic voltammetry (CV) was performed between 0.2 and 3.0 V at a scan rate of 0.5 mVs^{-1}. Electrochemical impedance spectra (EIS) were recorded at open-circuit potential over a frequency range from 10 kHz to 10 mHz with ac amplitude of 5 mV. All experiments were carried out at least twice to check reproducibility of the results. Representative results are only reported below.

3 Results and discussions

XRD pattern of the as deposited Sn film is shown in Fig. 1. Peaks are found matching with JCPDF reference CAS Number 04-0673 with tetragonal crystal structure. The (101) and (200) peaks at $2\theta \sim 32.3°$ and 30.8° are predominant. Relatively smaller (211) peak at 45.14° and (220) at 44.1° are also observed. The sharp peaks indicate that Sn film is well crystallized.

Typical SEM images of the as prepared Sn thin films are shown in Fig. 2. It is seen that a highly porous Sn film is formed under our experimental conditions of deposition. "Nano-beads" of size varying between 38 and 60 nm are present inside the porous structure, which are expected to provide a high surface area for the film (Fig. 2a inset). Figure 2b presents the cross-sectional view of Sn thin film on Si showing a thickness of ~ 2 μm for the Sn layer.

Figure 3a shows the CV of Sn film showing a pair of cathodic peaks at about 0.30 V and three anodic peaks in the potential region between 0.60 and 0.90 V. This data indicate that the RF-sputtered Sn film is electrochemically active with multistep lithiation and delithiation processes. The charge and discharge curves of Sn film electrode at a current density of 10 μA cm^{-2} are shown in Fig. 3b. On commencing charging, there is a sharp fall of potential to about 0.70 V, and thereafter there is a gradual decrease in potential. The charging is continued down to 0.10 V. Several potential plateaus present on the charging curve

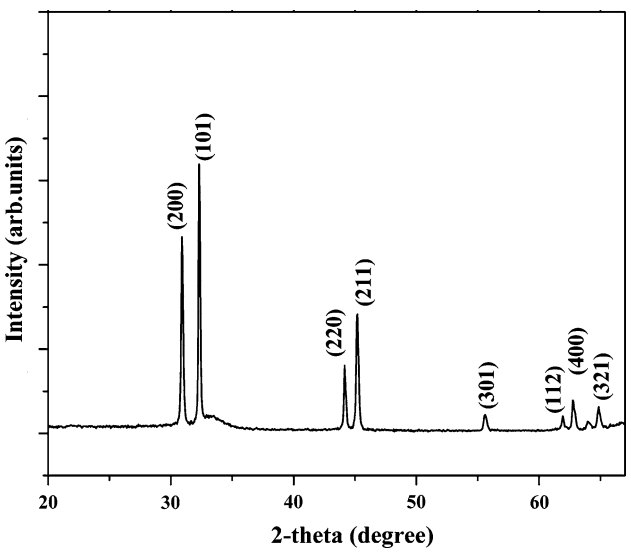

Fig. 1 XRD pattern of as deposited Sn thin film by RF-sputtering technique

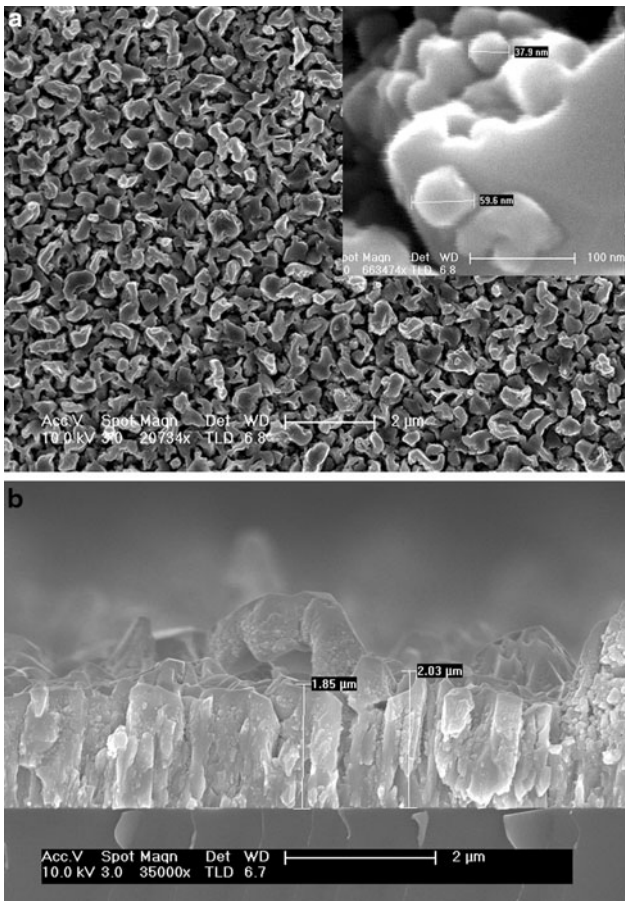

Fig. 2 **a** SEM surface micrographs of Sn thin film on Si, inset shown is magnified image. **b** Cross-sectional view of Sn on silicon substrate

suggest a multistage lithiation of Sn films. On discharging the electrode also, the potential is constant at different plateau regions suggesting multistep delithiation. There is an increase in potential at about 0.85 V. The discharge capacity obtained up to the potential limit of 1.2 V is 850 µAh cm^{-2}. Charge–discharge cycling of Sn film electrode was carried out for a few cycles and the data are presented in Fig. 3c. The discharge capacity is high in the 850 µAh cm^{-2} range during the first six charge–discharge cycles. The capacity starts decreasing thereafter and reaches a value as 278 µAh cm^{-2} at the tenth cycle.

The reaction between Sn and Li, which is an alloying and de-alloying type reaction, is written as:

$$_{x}Li^{+} +_{x} e^{-} + Sn \leftrightarrow Li_{x}Sn \ (0 \leq x \geq 4.4) \quad (1)$$

There are seven phases known to be formed between Li and Sn as Li_2Sn_5, LiSn, Li_7Sn_3, Li_5Sn_2, $Li_{13}Sn_5$, Li_7Sn_2 and $Li_{22}Sn_5$ [8, 13]. The thermodynamic and kinetic properties of these Li–Sn phases were investigated [14, 15]. Large volume changes occur during phase changes of these alloys. The phase that forms at the highest Li concentration ($Li_{4.4}Sn$) has a specific volume which is 283% of the volume of pure Sn. Thus, Li–Sn electrodes swell or shrink considerably when Li is added or removed. These volume changes occurring with different lithium concentrations in the particles result in pulverization of particles leading to a loss of electrical contact. It is the cause for capacity loss and poor cyclic performance.

During charging of the Sn thin film, Li^+ ions diffuse into the porous Sn film, resulting in the formation of Li–Sn alloys [16, 17]. For the purpose of this study, several Sn films were charged up to 0.67, 0.55 and 0.42 V (marked as asterisk symbol in Fig. 3b), and electrode properties were studied by SEM, XRD, XPS and EIS. The charge capacity values corresponding to these potentials are 154, 316 and 652 µAh cm^{-2}, respectively. The electrodes were removed from the cell, cleaned with acetone and dried before subjecting to these studies.

The XRD patterns of an as deposited Sn film and the electrodes charged up to the three potentials are shown in Fig. 4. On lithiation, the crystallinity of the Sn film is preserved but peak heights are altered. There is an increase in (200) peak and decrease in (101) peak compared with pure Sn film that is likely to be because of different stages of alloy formation. Also (112), (400) and (321) peaks of pure Sn film almost disappear for the Sn film lithiated up to 0.42 V. These observations throw light on formation of different phases of alloys formed between Sn and Li.

To examine the morphological changes occurring as a result of lithiation, SEM micrographs of the three samples were recorded and presented in Fig. 5. It is seen that as the lithiation progresses, cracks are formed because of expansion of the Sn film. From the high-magnification images (insets), it is seen that pulverization of Sn occurs on lithiation. EDX analysis of the elemental composition is shown along with the corresponding SEM image. It is seen that the amount of Sn decreases on increasing lithiation. The amounts of Li and oxygen increase from 0.67 to 0.42 V. F(K) and As (L) components are from electrolyte. Because Li cannot be detected by EDX, increase in oxygen amount is attributed to the presence of reactive Li on Sn surface forming lithium oxides as the lithiation progresses.

The XPS spectra recorded on Sn samples charged to the three lithiation potentials are shown in Fig. 6a–f. The values of binding energy, full-width half-maximum (FWHM) and atomic ratios of Sn $3d_{5/2}$ and Li 1s are compiled in Table 1. Sn $3d_{5/2}$ peak is deconvoluted into two components; peak around 484.6 eV matching to metallic Sn (Sn°) component and at 486.8 eV is because of oxidized Sn (Sn^{IV}) [18]. The oxide component dominates in intensity in Sn $3d_{5/2}$ peak. The Li 1s peak between 55 and 57 eV results from a mixture of lithiated compounds formed in the surface layer mainly consists of LiF and Li_2CO_3 components at 56 and 55.5 V, respectively (cannot be distinguished in the spectra because binding energies are close). When the

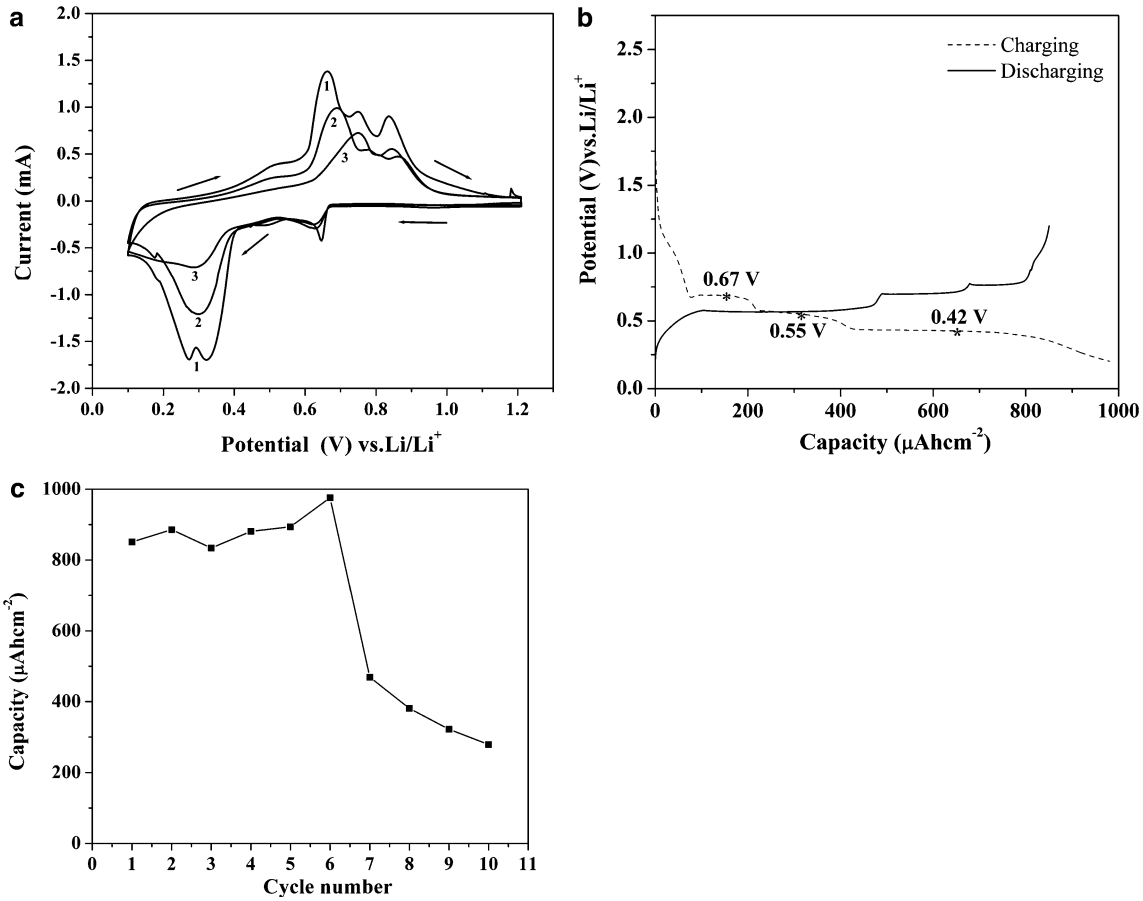

Fig. 3 **a** First three cyclic voltammograms recorded at 0.5 mV s^{-1} of a RF-sputtered Sn thin film. **b** Charge/discharge capacity obtained for a current density of 10 μAh cm^{-2}. **c** Specific capacity obtained as a function of cycle number

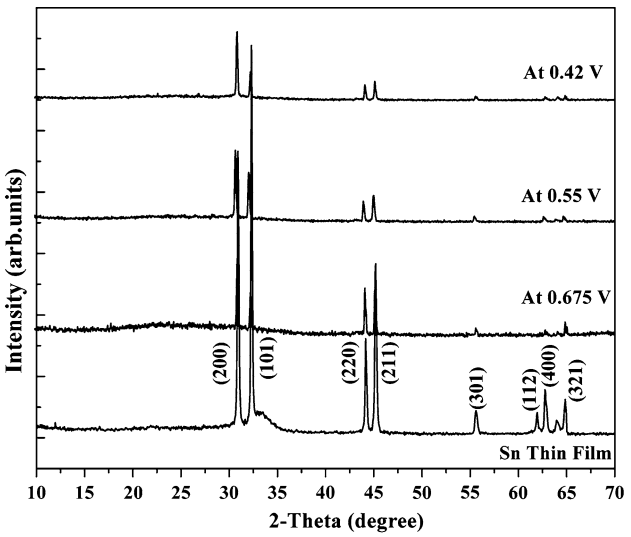

Fig. 4 XRD patterns obtained from Sn thin film lithiated to three different potentials along with as deposited Sn film for comparison

potential decreases lithiation of Sn film increases and hence atomic percentage of $Sn3d_{5/2}$ decreases to a low value of 1.7%, whereas Li 1s increases to 98.3%.

AFM 3D images of the as deposited Sn film and lithiated Sn films are shown in Fig. 7. It is seen that the topography of the films changes as lithiation progresses. The film attains increased roughness, which is reflected in the values of roughness factor (R_q). The value of R_q is 19 nm for the as deposited Sn film and it increases to 179 nm when the film is charged up to 0.67 V. R_q further increases to 206 nm for 0.55 V charged film and then to 315 nm for 0.42 V charged film. The progressive increase in R_q is attributed to the increase in volume of Sn layer because of formation of Li-rich Sn–Li alloy. Li^+ ions diffuse into the Sn film resulting in local expansion at these surface sites. With an increase in the quantity of Li^+ diffusing into Sn film, there is an increase in the roughness of the Sn surface.

AC impedance spectra of Sn film and lithiated Sn films recorded in the non-aqueous electrolyte are presented in Fig. 8. Although the impedance spectrum belongs to the cell consisting of Li and Sn electrodes, the changes in the spectra are considered to reflect the changes in electrochemical properties of Sn electrode. This is because the electrochemical reaction of Li electrode is fast and the cell properties are controlled by the Sn electrode. Each Nyquist

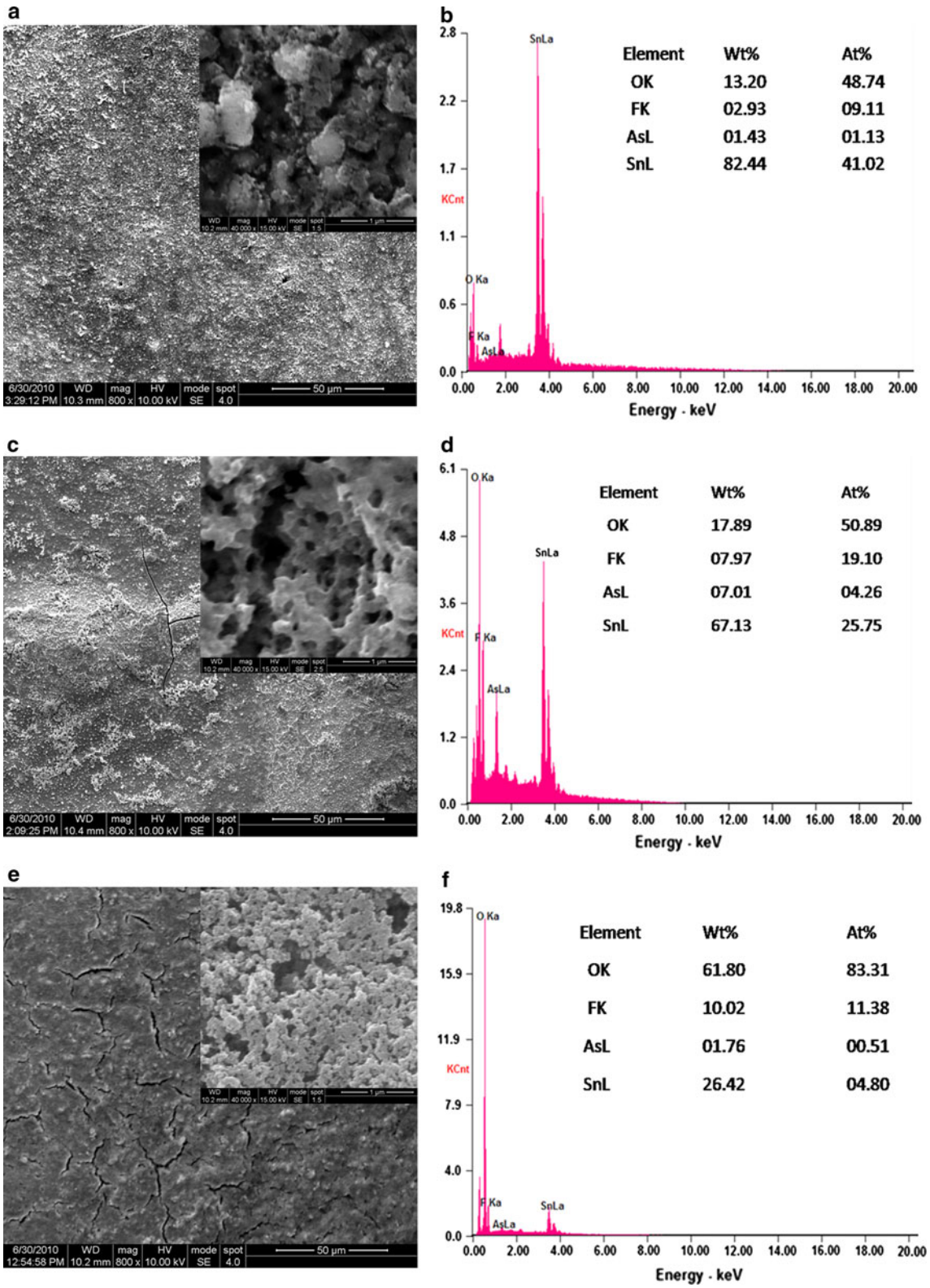

Fig. 5 SEM surface micrographs and corresponding EDX analysis of Sn thin film electrode at three different lithiation potentials, at 0.67 (**a, b**), 0.55 (**c, d**) and 0.42 V (**e, f**) (*insets* shown are magnified images)

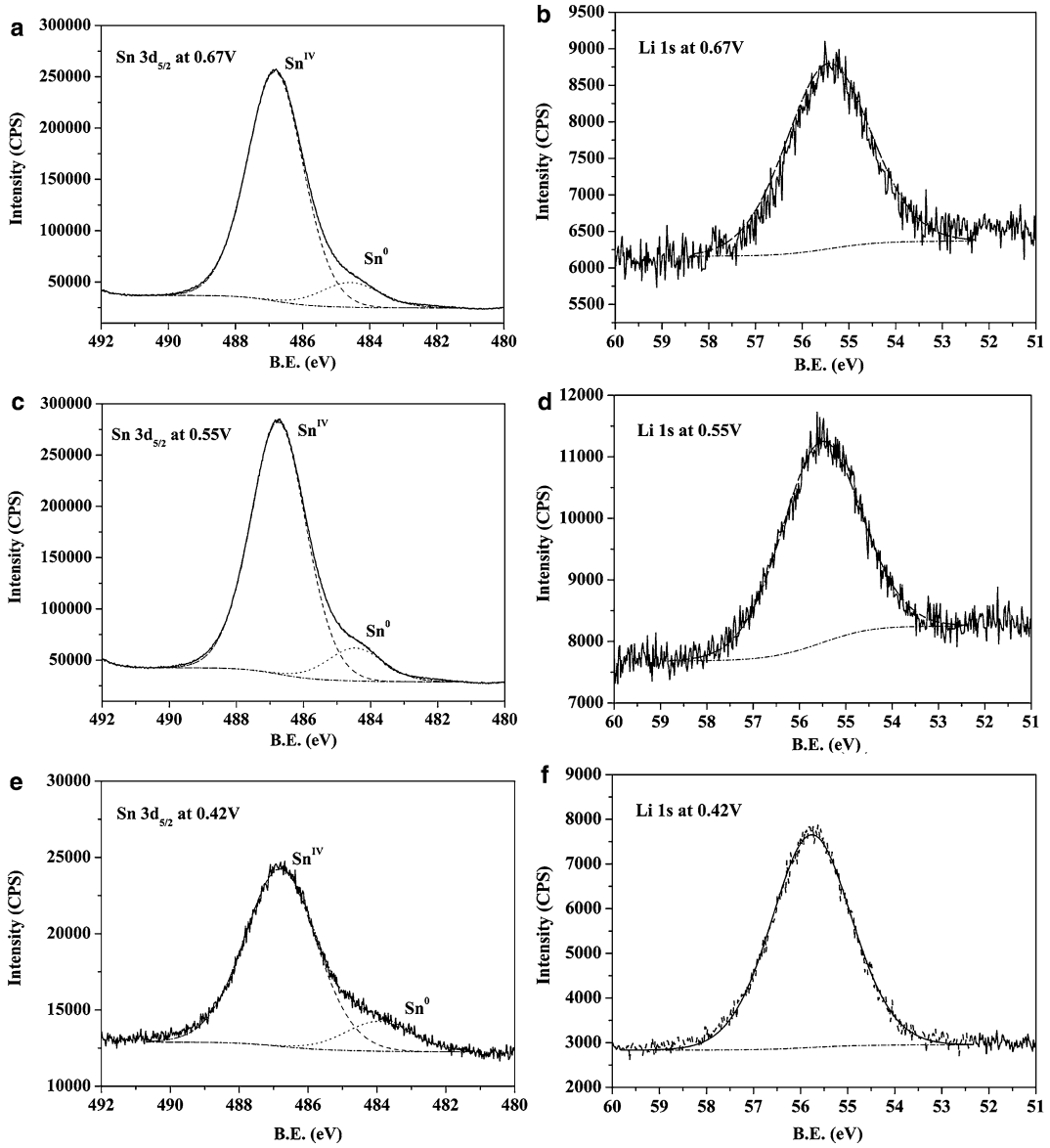

Fig. 6 XPS spectra of Sn thin film at three different lithiation potentials showing Sn $3d_{5/2}$ and Li 1s at 0.67 (**a, b**), 0.55 (**c, d**), and 0.42 V (**e, f**). Separate electrodes were employed, each being charged to the required potential

Table 1 Binding energy, full-width at half-maximum (FWHM) and relative atomic percentage (%) of Sn $3d_{5/2}$ and Li 1s on lithiation of Sn thin film

Lithiation potential (V)	Sn $3d_{5/2}$			Li 1s		
	B.E. (eV) Sn^{IV} Sn°	FWHM (eV) Sn^{IV} Sn°	Atomic % $Sn3d_{5/2}$	B.E. (eV)	FWHM (eV)	Atomic % Li 1s
0.67	486.8	1.9				
	484.6	2	30.7	55.5	1.5	69.3
0.55	486.7	1.9				
	484.4	2	27.3	55.6	1.6	72.7
0.42	486.8	2.4				
	484	2.2	1.7	55.7	1.8	98.3

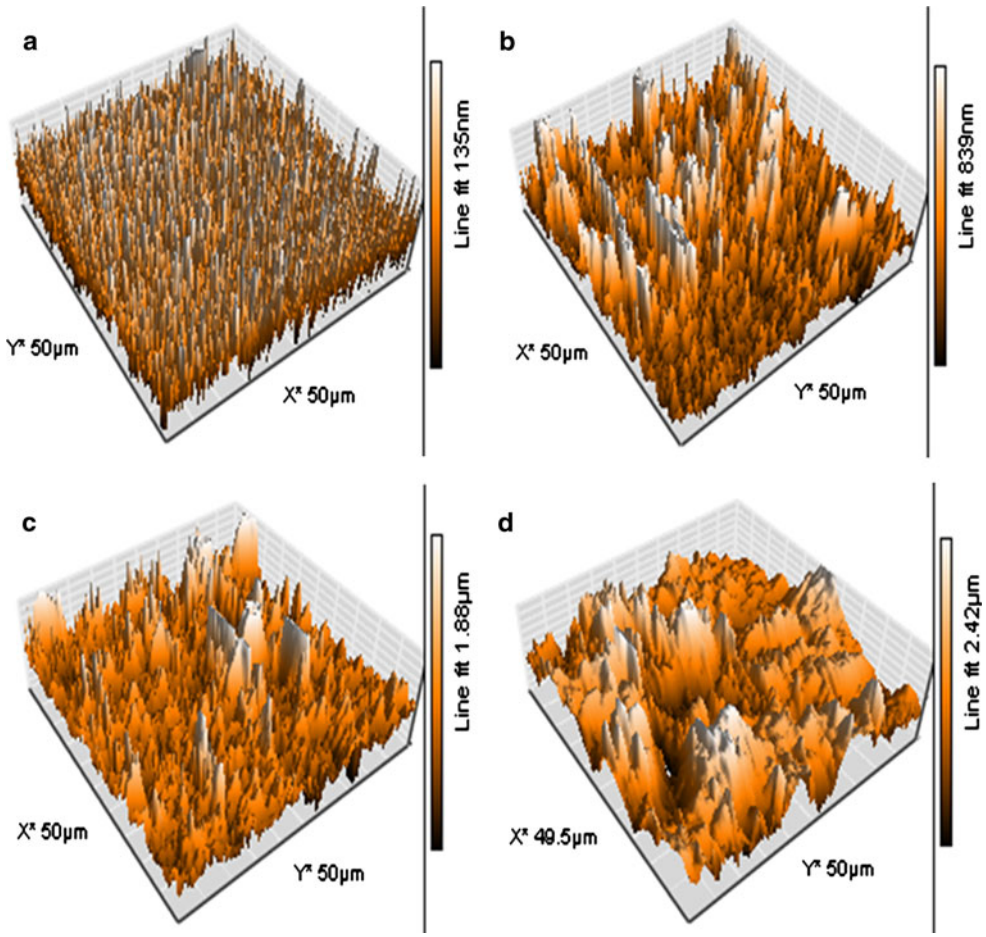

Fig. 7 AFM 3D images of as deposited (**a**) and lithiated Sn thin film at 0.67 V (**b**), at 0.55 V (**c**) and 0.42 V (**d**)

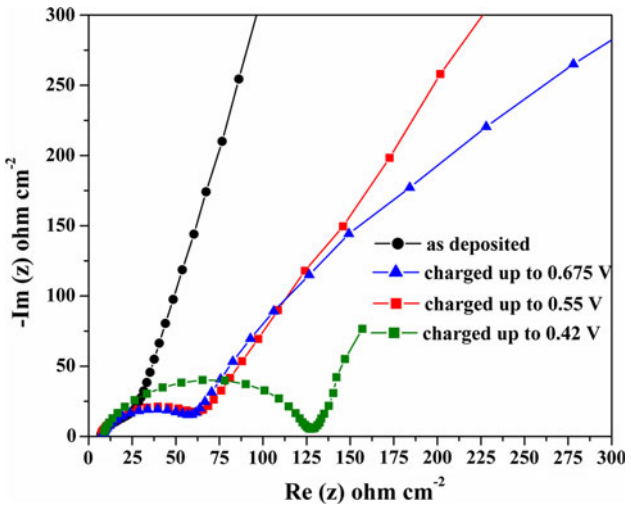

Fig. 8 AC impedance spectra recorded from as deposited and lithiated Sn thin film

impedance spectrum consists of a high-frequency intercept on *x*-axis, a semicircle followed by a linear tail at low frequency. The diameter of the semicircle provides charge transfer resistance (R_{ct}) of the process of lithiation of Sn film. It is found that the values of R_{ct} are 45, 66, 74 and 112 Ω, respectively for the 0.67, 0.55 and 0.42 V charged Sn films. These data indicate that the lithiation process becomes more and more sluggish as the quantity of Li increases in the Li–Sn alloy films.

4 Conclusions

Physicochemical changes responsible for reduced capacity retention of Sn thin film anode were investigated in detail. Thin films of Sn were deposited on Pt/Si substrate by RF-sputtering method, and they were subjected to the electrochemical lithiation. The electrodes charged to different potentials were examined by several physicochemical methods. It was found that the increased quantity of Li in Li–Sn alloy films reflected in increasing roughness factor, which resulted in film fractures and pulverization. Increase in R_{ct} values obtained from EIS studies indicated a sluggish lithiation process with increased potential.

Acknowledgments This work was funded by Defense Research Development Organization (DRDO), Government of India.

References

1. Bates JB, Gruzalski GR, Dudney NJ et al (1994) Solid State Ionics 70/71:619
2. Ji HJ, Kang SH, Lee HJ et al (2009) Proc IMechE Part G J Aerospace Engineering 223:107
3. Liu WY, Fu ZW, Qin QZ (2007) Thin Solid Films 515:4045
4. Jeon EJ, Shin YW, Nam SC et al (2001) J Electrochem Soc 148:A318
5. Navone C, Hadjean RB, Pereira Ramos JP et al (2009) J Electrochem Soc 156:A763
6. Winter M, Besenhard JO (1999) Electrochim Acta 45:31
7. Du Z, Zhang S, Jiang T et al (2010) Electrochim Acta 55:3537
8. Courtney IA, Dahn JR (1997) J Electrochem Soc 144:2943
9. Hamon Y, Brousse T, Jousse F et al (2001) J Power Sources 9798:185
10. Tamura N, Ohshita R, Fujimoto M et al (2002) J Power Sources 107:48
11. Lee SJ, Lee HY, Jeong SH et al (2002) J Power Sources 111:345
12. Chiu KF, Lin HC, Lin KM et al (2006) J Electrochem Soc 153:A920
13. Courtney IA, Dahn JR (1997) J Electrochem Soc 144:2045
14. Wen CJ, Huggins RA (1981) J Electrochem Soc 128:1181
15. Wen CJ, Huggins RA (1980) J Solid State Chem 35:376
16. Thackeray MM, Vaughey JT, Johnson CS et al (2003) J Power Sources 113:124
17. Timmons A, Dahn JR (2006) J Electrochem Soc 153:A1206
18. Naille S, Dedryvere R, Martinez H et al (2007) J Power Sources 174:1086